THE BALTIC JOURNAL OF ROAD AND BRIDGE ENGINEERING
2024/19(4)

ISSN 1822-427X/eISSN 1822-4288
2024 Volume 19 Issue 4: 1–27
https://doi.org/10.7250/bjrbe.2024-19.646

THE PERFORMANCE OF DIFFERENT FREIGHT WAGON BOGIE TYPES ON A SMALL RADIUS CURVE – COMPARISON OF FIELD MEASUREMENTS AND SIMULATIONS

TIIA-RIIKKA LOPONEN*, RIZWANULLAH SHAIK, RIKU VARIS, HEIKKI LUOMALA, PAULI KOLISOJA

Research Centre Terra, Faculty of Built Environment, Tampere University, Tampere, Finland

Received 8 May 2024; accepted 4 October 2024

Abstract. The running performance of different freight wagons affects the damage they cause to the track, which in turn influences the maintenance costs of the track. The track access charges may be imposed based on the track friendliness of a wagon if the features of the wagons are known. In Finland, besides the structure of the bogies, the width of the bogies also varies since some of the bogies are designed for a track gauge of 1524 mm and some for a track gauge of 1520 mm. In this paper, the performance of different freight wagon bogies on a small radius curve is investigated by means of field measurements and simulations. Wheel-rail contact forces and angle of attack values of six different wagon types are measured. In addition, simulations are created to gain further knowledge on wheel-rail contact forces, angle of attack values, and wear values. Based on this research, it would be beneficial to use a wider track gauge in small radius curves to make the curve negotiation easier for some bogie types. It was also noticed that a small radius curve with only

* Corresponding author. E-mail: tiia.loponen@tuni.fi

Tiia-Riikka LOPONEN (ORCID ID 0000-0002-7305-0178)
Riku VARIS (ORCID ID 0000-0001-8375-2950)
Heikki LUOMALA (ORCID ID 0000-0002-7113-3527)
Pauli KOLISOJA (ORCID ID 0000-0001-7709-180X)

a short transition zone could be very risky regarding derailment potential, especially for empty wagons.

Keywords: angle of attack, derailment risk, freight wagon bogie, multibody dynamics, track gauge, track friendliness, track curve, vehicle model, wheel-rail contact, wheel force.

Introduction

The rolling stock bogies used for freight transportation are quite different when compared to the more sophisticated bogies used for passenger transport. The ability of the vehicles to negotiate curves depends on many factors like the construction of the bogie and the maintenance regimen of the freight wagon bogie. The forces imparted by the freight wagon bogies are prone to causing different types of damage to the track, and it is necessary to obtain reliable knowledge about that behaviour to be able to determine the appropriate track access charges in the future. With impending demands to increase the axle loads, there is an increasing need to study the loading behaviour of different freight wagon bogies on the existing infrastructure. This paper investigates freight wagon bogies running on small radius curves by measuring the wheel-rail forces and angle of attack (AOA). The ability of the bogies to steer in small radius curves is also studied by means of simulations with a freight wagon model; in addition to the wheel-rail contact forces and angle of attack, the amount of wear in wheel-rail contact is also being estimated.

The Finnish railway network runs on the broad-gauge track with a gauge of 1524 mm. A diverse fleet of freight wagon bogies runs on the network with maximum axle-load limits between 20–25 tons (Finnish Transport Infrastructure Agency, 2024). The nominal width of the bogies varies by 4 mm since most of the bogies running in Finland are designed for a 1524 mm track gauge, while some are designed for a 1520 mm track gauge. Since many types of bogies run on the Finnish rail network, it is important to know the running performance of different bogies. If the track loads typical of different freight wagons are known, the track access charges could be determined according to the probable corresponding track damage, which would favour track-friendly wagons. This goal led to the need for measuring the lateral forces on the rails caused by the passage of different types of freight wagons. The measurement activity was devised in the summer of 2022 to measure the wheel-rail forces for a fleet of freight wagon bogies in the Kouvola railway yard. Unlike the normal track section, railway yard tracks generally have a smaller curve radius and no transition curves which may lead to a greater amount of lateral forces in wheel-rail contact, and, for that reason, a higher risk of derailment and wear rate. Different freight wagon bogies, such as the 18-100 bogie, Y25 bogie, Axle Motion III (K17) bogie, link suspension bogies K14 and K16, and the single-axle UIC double link suspension freight wagon bogie, were tested. Vertical and lateral forces were recorded, and the angle of attack was also measured to observe the behaviour of the wheel along the outer rail of the curve. These measurements are part of the initial research phase of a larger project, where the track friendliness of different freight wagons will be determined. The main part of that project is to produce different freight wagon bogie models in order to simulate the behaviour of freight wagons and gain reliable knowledge to adjust track access charges. Some results from the previously built 18-100 bogie model are also presented in this paper. With the help of these field measurements and freight wagon simulations, our understanding of the freight wagon bogies and their behaviour moving on small radius curves can be expanded.

1. Curving performance of freight wagon bogies

The damage to the track is caused by the load imparted by the bogies. Such loading behaviour results in wear-causing damage that eventually reduces the service life of the rails. In addition, dynamic loading causes ballast fouling, deteriorates the track geometry, and imparts vibrations to the immediate surroundings. A bogie that is able to negotiate any track conditions is said to be track-friendly if it produces low/moderate forces with less damage and wear to the tracks. Such a bogie will cause minimal track deterioration, incur less maintenance and renewal activities, reduce the associated costs, and result in favourable operating vehicle conditions (Orvnäs et al., 2007).

The forces between the wheel and the rail are distributed in vertical, lateral, and longitudinal directions. The position of the wheel-rail contact on the running surface affects the distribution of the forces transmitted by the wheel onto the rail. When a bogie negotiates a larger curve radius section, the conical wheels create a difference in the rolling radius between left and right wheel, which will typically induce steering forces and yaw moments that align the bogie to a more radial position. The wheelset shifts sideways to allow the outer wheel to run with a larger rolling radius than the inner wheel. The resulting longitudinal creep forces at the wheel-rail interfaces on wheels of the same axle form a moment that steers the bogie around curves (Wu & Wilson, 2006). The yaw moment depends on the values of longitudinal creep forces, which are typically higher with the leading wheelset (Arias-Cuevas et al., 2010). As the curve radius decreases, the bogie suffers from what is called an understeer, where the leading wheelset of the bogie tends to run in flange contact with the outer rail of the curve (Thompson, 2009). It has been noticed that on a small radius curve, the lateral forces on the leading wheelset are higher than the lateral forces on the trailing wheelset (Weilguny et al., 2024). Lateral creep occurs in rolling contact in the presence of an angle of attack (Vollebregt et al., 2021). The angle of attack of the leading wheelset is high when executing such small radius curves due to the wheelset attempting to move ahead but being constrained to move along the curve radius by flanging. A lateral slip is induced at the wheel-rail contact patch, giving rise to wear and rolling contact fatigue (RCF) at the wheel tread and rail head, and it can also lead to a potential flange-climbing phenomenon that causes the bogie to derail (Hiensch et al., 2018).

In small radius curves, the track gauge may be intentionally widened to gain more rail clearance or lateral space for the wheelset to negotiate a curve (Figure 1). Wear in both the wheel and rail also increases the value of rail clearance. Gauge widening in small radius curves can reduce the lateral forces significantly, especially on the trailing wheelset (Weilguny et al., 2024).

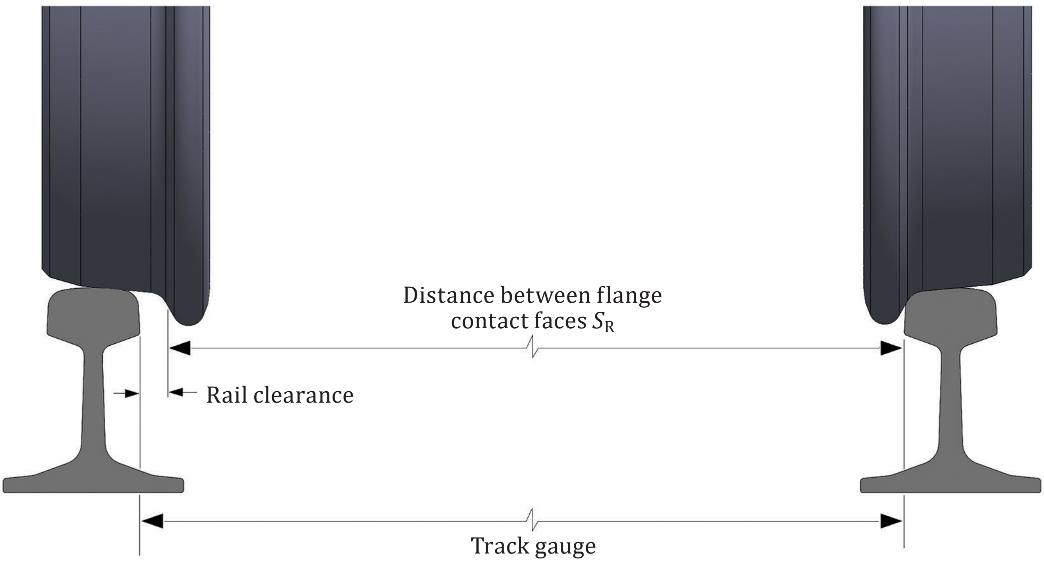

Figure 1. Rail clearance depends on the track gauge and wheelset dimensions

The dimensions and yaw stiffness of a freight wagon bogie, as well as the clearance between the wheel and rail, play an important role in the bogie's curving performance. For example, the distance between two wheelsets in a bogie and the yaw stiffness varies from one bogie to another. The nominal value for the distance between flange contact faces (S_R) in Finland is 1510 mm for most of the bogies, but 1506 mm for a small group of bogies. For that reason, an 18-100 bogie is a bit narrower (S_R = 1506 mm) than other bogies (S_R = 1510 mm) that were measured in Kouvola. Therefore, the 18-100 bogie has more space to move laterally (bigger rail clearance), which may affect the results.

One of the most common bogies in Europe, the Y25 bogie, has a non-smooth characteristic (Solčanský, 2021). It typically has a longitudinal clearance of roughly 4 mm, which allows the bogie to negotiate the curve to a certain degree. However, as soon as the clearance is exceeded, the stiffness in the longitudinal direction rises steeply, leading to unavoidable flanging in the outer wheels (Jönsson, 2007). In a comparative study implemented by Stichel (1999), the steering performance of the Y25 bogie was adequate only until a 600-metre curve radius, whereas the link bogies show adequate steering performance until a 300-metre curve radius due to its soft longitudinal primary suspension.

Müller (2001) reported the results of a series of dynamic tests carried out with the Y25 and K17 bogies. The tests were conducted on the tangent and curved (curve radius less than 600 m) sections with varying axle loads. It was observed that the vertical force of the K17 bogie was lower than the vertical force of the Y25 bogie even though the axle load of the K17 bogie was greater. The reason for such behaviour was attributed to the softer suspension characteristic of the K17 bogie. These bogies have clearances of up to 9 mm in the longitudinal direction.

The 18-100 three-piece bogie is often prone to warping or lozenging where the bogie is out of shape (shape of parallelogram), causing both the leading and trailing wheelsets to adopt higher angle of attack values and emit wheel squealing (RISSB, 2021). The leading wheelset, which runs at an angle of attack, is forced to slip laterally as it moves forward, producing extra running resistance and extra wear on wheels and rails (Jönsson, 2007). In the paper by Boronenko et al. (2006), it was reported that the flange wear rate of the 18-100 bogie is about 11.1 mm per 100 km when compared to the tread wear of 3.6 mm per 100 km for wagons running in laden conditions. Such behaviour was observed for bogies running in curves with a radius less than 600 m. Again, the importance of the longitudinal clearance between the axle box and the side frame was pointed out, especially in curves with clearances less than 8 mm where there was a steep increase in the angle of attack and wear and an increase in the Y/Q coefficient.

In this study, an effort is made to understand the curving behaviour of these freight wagon bogies by measuring the wheel-rail forces and the angle of attack of the passing wheelsets on a small curve radius. Furthermore, the freight wagon performance in curved track sections has been analysed through simulations.

2. Field measurements

Real-time measurements offer a deeper understanding of the loading phenomenon and the performance of different freight wagon bogies. The underlying curiosity about studying the distribution of wheel-rail forces and steering capability in such tight running conditions led to the measurements of freight wagon bogies running on the Finnish rail network. The train fleet consisted of different freight bogies, both with the loaded and unloaded configuration, to run through a curve with a 200-metre curve radius in the Kouvola railway yard in southern Finland.

The forces of different freight bogies were measured at the Kouvola railway yard on a test track consisting of 54E1 rail profiles laid on wooden sleepers with 1:40 inclined Hey-Back fastening system. Figure 2 depicts two measurement sections (1 and 2) that were selected along the curve radius of the test track with varying track gauges and different rail side wear profiles. The first measurement section had a track gauge of 1535 mm (“wide gauge curve”) with a side wear of the outer rail between 2 and 5 mm. The second measurement section was chosen along the part of the curve that underwent maintenance recently. The rails were changed to new ones, but the sleepers and the fastening system remained the same. After the maintenance, the track gauge at this section was 1530 mm (“narrower gauge curve”) and there was no indication of any wear on the rails. The lateral stiffness of the track was assumed to be similar in both old and new track sections. The selection of such sections along the curve makes it possible to understand the effect of varying track gauges and estimate the amount of force at different stages of the curve radii.

The track gauges are far from the nominal 1524 mm because compensation has been provided for any bogie to negotiate a very small curve radius. The cant was measured along the test track, and it was found that the outer rail was surprisingly lower than the inner rail in the range of 5–35 mm. At the beginning of the curve, the cant changes abruptly by 18 mm on the lower side for the outer rail over a distance of 6.1 m. Such a change could contribute to the risk of a derailment scenario due to a wheel-load imbalance. This negative cant also means that there is a clear cant deficiency, which generates additional lateral forces as a result of the non-compensated centrifugal forces (Diana et al., 2016). The rail profiles and wheel profiles were measured using a CALIPRI measurement device.

Each measurement section has four sensors on the outer rail measuring the lateral force as it was of principal interest (M1-M4 in Figure 2), and two sensors on the inner rail measuring the same quantity (M5 and M6 in Figure 2). Vertical forces were obtained from M2 and M3 for the outer rail and at M5 and M6 for the inner rail. To measure the angle of attack of a wheelset, a laser sensor pointing to the railhead of the outer rail was installed at R1 (Figure 2) along with a high-speed camera to record the wheel passages.

Different measurement techniques for the lateral and vertical forces were tested, and the following methodology that gave the most reliable measurement results was adopted. The vertical forces were measured by attaching the strain gauges to the web of the rail at 45-degree angles, so that the actual measured parameter was the shear force of the rail. When measuring the shear force, the bending moment and the twist of the rail do not affect the results, which is the main reason for choosing this method. The gauges were glued onto the web of the rail along the neutral axis on both sides of the rail completing the strain gauge full bridge. The lateral forces were also measured using the shear force method, and strain gauges were glued onto the foot of the rail at 45-degree angles (Figure 3a). The measurement technique with shear force is similar to the so-called base chevron configuration method, which, according to literature (Powell & Gräbe, 2017), is more accurate in measuring the lateral forces compared to the web-bending

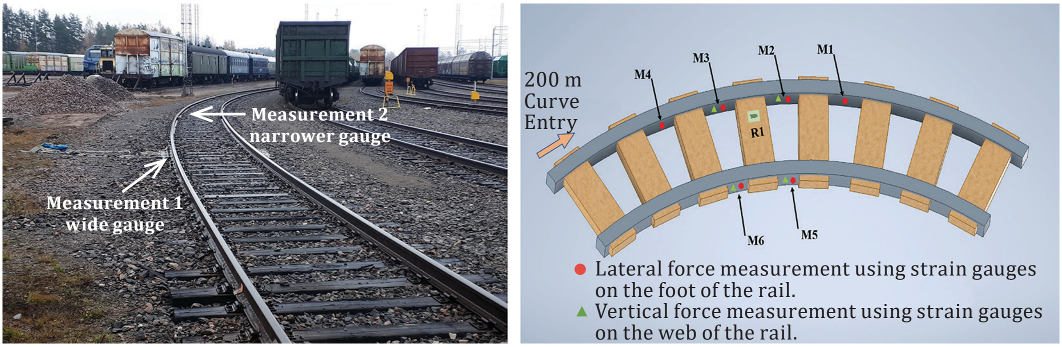

Figure 2. Left: Measurement site at the Kouvola railway yard; Right: Setup of the force sensors (M1-M6) and the laser sensor (R1) along the curve

configuration method, wherein the gauges are attached in a vertical orientation along the web of the rail. Both the measurement sections had a similar set-up for finding the lateral and vertical forces. Since lateral forces were of particular interest, each measurement section had four data points on the outer rail.

The strain gauges used for measuring the forces were calibrated before the tests using a hydraulic jack and a load cell. The setup for the calibration of the vertical force is shown in Figure 3b and the calibration of the lateral forces in Figure 3c. The calibration of the sensors was carried out with such accuracy that the measurement error of the entire system was less than 5%. The data obtained from the strain gauges was processed using the data acquisition system NI 9237 from National

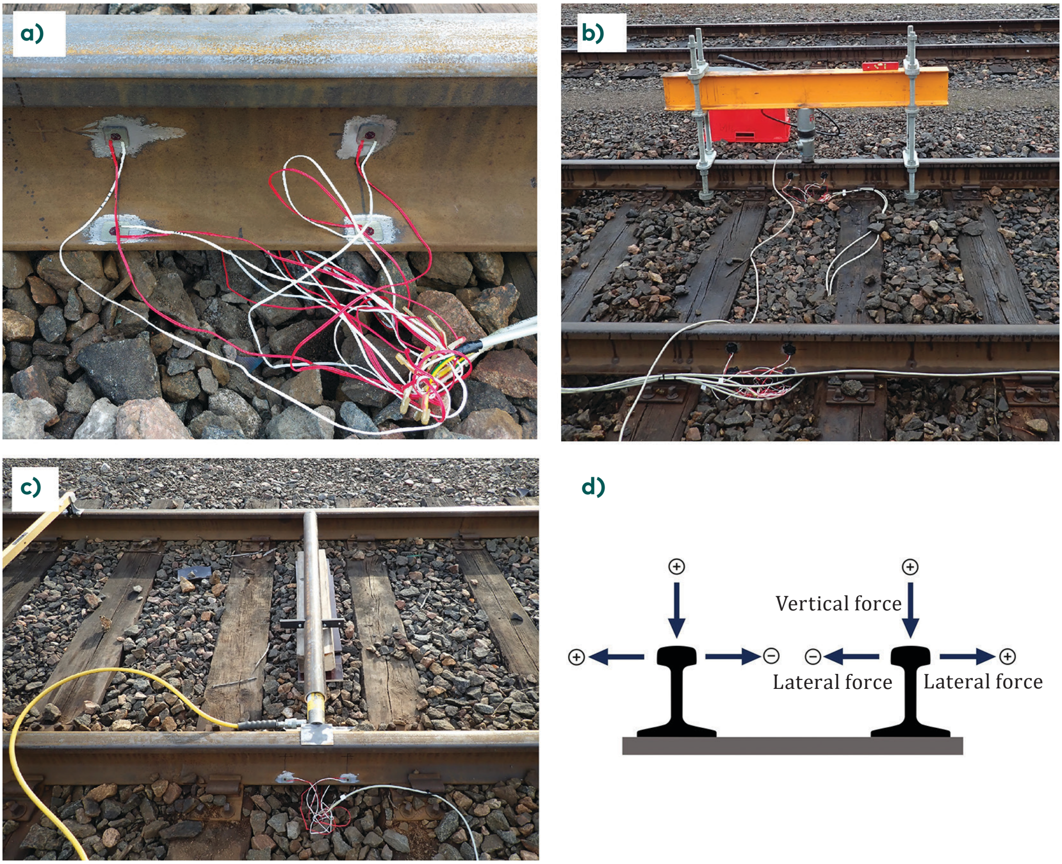

Figure 3. (a) Strain gauges glued onto the web and foot of the rail; (b) Calibration rig for vertical forces; (c) Calibration rig for lateral forces; (d) Sign convention for the wheel-rail forces

Instruments with a sampling rate of 5 kHz. For the sign convention, any component of the lateral force that was pushing towards the outside of the rail was considered positive while any force pulling the rail to the middle of the track was taken to be negative. A downward pushing force between the wheel and the rail is considered positive in terms of vertical forces (Figure 3d).

In addition to wheel-rail forces, the angle of attack was measured using a laser sensor to study the ability of the vehicle to undertake such a small curve radius. At both measurement sections, the angle of attack was measured along the outer rail of the curve to understand how big the yaw angle of the wheelset is with respect to the track. A sign for the angle of attack value was considered negative when the wheelset did not fully follow the curve. A wayside measurement system, which was used in this study, was adopted from the experiments conducted by Milković et al. (2015, 2017). The method was chosen because it easily provides the angle of attack information for all the wheels passing along the track.

A Panasonic HL-G112-S-J laser sensor with a measurement centre distance of 120 mm and a sampling rate of 5 kHz was used at both measurement sections. The sensor (R1 in Figure 4) was positioned in such a way that the laser beam was pointed above the top of the rail to effectively obtain a sufficient measurement section on the slope. The laser sensors were bolted to a specially designed frame, which were then fastened onto the wooden sleepers, as shown in Figure 4. High-speed cameras were also placed to obtain footage of the wheel passages to identify wheels that were in flange contact with the rail.

The tests were carried out for five different freight wagon bogies and for one freight wagon with two single axles (Table 1).

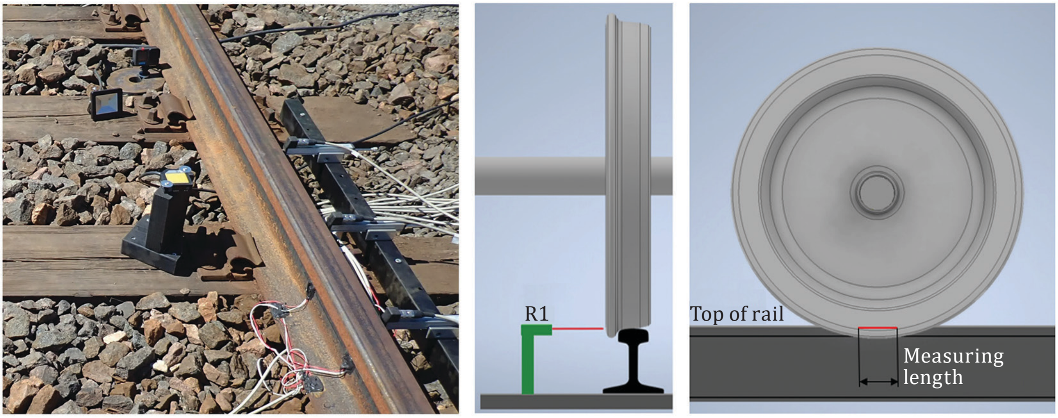

Figure 4. Left: Laser sensor position along the outer rail; Right: Laser sensor (R1) and its measurement principle

Table 1. Freight wagon bogies tested at the Kouvola railway yard

No.	Bogie type	Load scenario	Axle weight, kN
1	K14	Empty	54
2	K16	Loaded / empty	215 / 65
3	K17	Loaded / empty	218 / 74
4	UIC double-link single axle bogie	Loaded /empty	198 / 72
5	Y25	Loaded	209
6	18-100	Loaded	215

In the summer of 2022, the measurements were carried out in dry weather conditions. The fleet that was tested was comprised of fully loaded and empty wagons to see the differences in the forces. The freight wagon bogies were pulled and pushed by locomotives at different velocities – 5 km/h, 15 km/h, 25 km/h, and 35 km/h. Therefore, for each velocity scenario, two datasets of signals would come from the strain gauges and laser sensors. The test velocity for the fleet was achieved as close as possible by the test train drivers during the measurement. The distance between two sensors was also measured to calculate the running velocity of the fleet from the signals obtained from the sensors with more accuracy.

3. Measurement results

The data obtained from both measurement sections was analysed to determine the lateral and vertical forces using proper calibration factors on the FlexPro analysis software. It was noted that the four different measurement points measuring lateral forces produced a slight variation of results; therefore, the highest lateral force of those results was selected for the analysis. Using the data of both the lateral forces (Y) and vertical forces (Q), the derailment coefficient (Y/Q) was calculated for wheels passing on the outer rail. The Y/Q derailment ratio is generally used to evaluate the vehicle safety, wherein according to the UIC 518 standard, a ratio above 0.8 could lead to potential derailment in curves where $R \geq 250$ m (UIC 518, 2005). Hence, the curve in these tests was even tighter than in the UIC definition. During the measurement, the outer wheel of the leading wheelset was almost without exceptions flanging, and this was recorded using the high-speed cameras. As a result, the wheel squeal was observed for some of the freight wagon bogies. Such running conditions (small curve radius) would generate large Y/Q ratios of the flanging wheel of the bogie's leading wheelset due to the angle of attack of the wheelset (Diana et al., 2016).

The principle of determining the angle of attack is shown in Figure 5. The signal obtained from the sensor is shown where the leading wheelsets of the bogies (axles 1 and 3) appear to have a sloped angle, confirming the steering action with the trailing wheelsets (axles 2 and 4) following up along the curve (almost negligible slope). If the angle of attack is nearly zero, the slope of the line obtained from the laser (blue line in Figure 5) is almost zero and the line is almost horizontal.

The angle of attack is obtained by transforming the signal from the time domain into the spatial domain, and then the slope is calculated using a simple linear regression technique. During the calculation, only the central part of the signal obtained from the sensor is used, neglecting other regions to get more precise values of the slope.

The data was tabulated for all the individual wheels of the freight wagon bogies and then assessed to identify the wheelsets that gave the highest and lowest forces. Table 2 shows the results of the lateral forces in a curve for bogies with different velocities. The results shown in Table 2 are for the outer wheel of the leading wheelset, which has the highest values. Table 2 also shows the comparison between measurement section 1 (wide gauge curve) and measurement section 2 (narrower gauge curve).

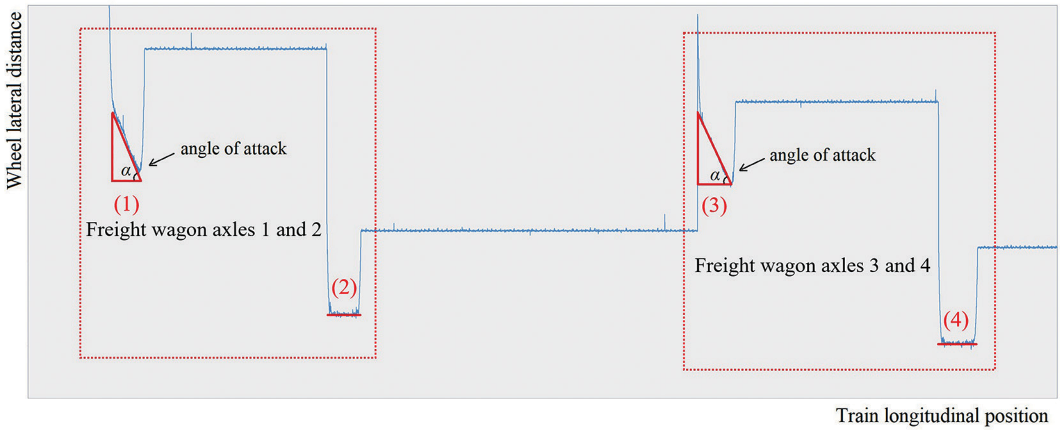

Figure 5. Example of an AOA signal (blue line) recorded while the wheels of freight wagon bogies are passing the laser sensor. Bogie 1 (axles 1 and 2) and bogie 2 (axles 3 and 4) are surrounded by squares (red dashed line). The wheels cause a sudden change in the laser signal level and the angle of attack of the wheelset can be calculated from the slope of the signal (red)

Table 2. (Left) The highest lateral forces from measurement section 1 (wide gauge curve); (right) The highest lateral forces from measurement section 2 (narrower gauge curve) – outer wheel of the leading wheelset negotiating the curve. UL represents empty wagon and L represents loaded wagon (all numbers are in kN). The scale of the colours is 0 (green) – 50 (orange) – 100 (red).

Lateral force, kN, wide gauge curve				
Bogie Type	**5 km/h**	**15 km/h**	**25 km/h**	**35 km/h**
$K14_{UL}$	5.19	4.49	6.21	8.12
$K16_{UL}$	4.35	4.59	7.06	8.04
$K17_{UL}$	20.25	20.14	19.11	17.21
Two-axle$_{UL}$	10.72	9.13	13.40	13.66
$K16_{L}$	13.47	14.63	22.08	34.45
$K17_{L}$	46.79	44.15	44.03	45.38
$Y25_{L}$	64.01	59.89	57.87	59.77
18-100$_{L}$	54.37	56.37	62.29	62.43
Two-axle$_{L}$	20.93	26.58	30.48	32.98

Lateral force, kN, narrower gauge curve				
Bogie Type	**5 km/h**	**15 km/h**	**25 km/h**	**35 km/h**
$K14_{UL}$	4.37	2.69	4.97	7.49
$K16_{UL}$	12.96	11.11	14.86	15.58
$K17_{UL}$	22.76	25.44	25.87	28.00
Two-axle$_{UL}$	16.45	13.10	17.61	19.99
$K16_{L}$	56.69	59.83	63.70	75.98
$K17_{L}$	53.29	62.44	67.70	68.53
$Y25_{L}$	60.72	59.98	60.24	55.89
18-100$_{L}$	53.98	63.22	67.33	69.75
Two-axle$_{L}$	51.45	38.05	35.78	48.88

As stated above, the outer wheel of the leading wheelset has the highest magnitude of the lateral force, which usually increases with increasing velocities. The loaded wagons have higher lateral forces compared to the empty wagons. The leading axles of the $K16_L$, $K17_L$, and 18-100$_L$ bogies show the highest lateral forces, especially at the test velocity of 35 km/h in the narrower gauge curve. The $K16_L$ bogie caused very high lateral forces in the narrower gauge curve, while in the wide gauge curve, the lateral forces of the $K16_L$ bogie were significantly lower. This may be due to the lack of flange contact in the wide gauge curve, but, unfortunately, during that wagon passage, the high-speed cameras were not working well enough to confirm whether there was a flange contact or not.

In the case of the empty wagons, the $K17_{UL}$ bogie had the highest lateral force values. The lateral force was especially high in the narrower gauge curve at the test velocity of 35 km/h.

The centrifugal forces in a curve depend highly on the velocity of the wagon. The centrifugal forces for bogies with different velocities in a curve with radius R = 200 m are calculated and shown in Table 3.

Table 3. Calculations of the lateral force caused by the centrifugal force in a curve with radius R = 200 m. The scale of the colours is from 0 (white) to 10 (red).

Lateral centrifugal force, kN				
Bogie Type	**5 km/h**	**15 km/h**	**25 km/h**	**35 km/h**
$K14_{UL}$	0.05	0.48	1.33	2.60
$K16_{UL}$	0.06	0.58	1.60	3.13
$K17_{UL}$	0.07	0.66	1.82	3.57
Two-axle$_{UL}$	0.07	0.64	1.77	3.47
$K16_{L}$	0.21	1.90	5.29	10.36
$K17_{L}$	0.21	1.93	5.36	10.51
$Y25_{L}$	0.21	1.85	5.14	10.07
18-100$_{L}$	0.21	1.90	5.29	10.36
Two-axle$_{L}$	0.19	1.75	4.87	9.54

As it is obvious from basic physics, centrifugal forces shown in Table 3 increase as the velocity and wagon weight increase. However, even with the velocity of 35 km/h, the centrifugal force is only a small part of the overall lateral force, which can be seen in Table 2. This means that other factors affect the lateral force value more than centrifugal forces.

Overall, the lateral forces are a bit higher in the tighter section (measurement section 2), and Table 4 shows this difference (as percentages) between the lateral forces.

Table 4. Difference in lateral forces between two measurement sections (wide gauge curve vs. narrower gauge curve) for the leading wheelset (left wheel) of different freight wagons (as percentages). The scale of the colours is from −100 (blue) to 100 (red)

Difference in lateral forces, %				
Bogie type	**5 km/h**	**15 km/h**	**25 km/h**	**35 km/h**
$K14_{UL}$	−15.80	−40.09	−19.97	−7.76
$K16_{UL}$	197.93	142.05	110.48	93.78
$K17_{UL}$	12.40	26.32	35.37	62.70
Two-axle$_{UL}$	53.45	43.48	31.42	46.34
$K16_{L}$	320.86	308.95	188.50	120.55
$K17_{L}$	13.89	41.43	53.76	51.01
$Y25_{L}$	−5.14	0.15	4.10	−6.49
18-100$_{L}$	−0.72	12.15	8.09	11.73
Two-axle$_{L}$	145.82	43.15	17.39	48.21

Although there is some increase in the lateral forces for most of the freight bogies in Table 4, both empty and loaded K16 bogies have the highest difference between both measurement sections in all velocities. Therefore, the track gauge plays an important role for that specific bogie, but not that much for the other bogies. However, based on these results, it would be beneficial to use a wider track gauge in small radius curves to make the curve negotiation easier for some bogie types.

The distribution of lateral forces depends on the flexibility of the primary suspension, the yaw stiffness of the bogie, and the non-compensated centrifugal force coming from the weight of the wagon. In the narrower gauge curve, the wheels have less room to fully negotiate the curve, thereby running in flanging condition for the leading wheelset. However, in this type of a small radius curve, it is likely that flange contact also appears in a wider track gauge. As the 18-100 bogie is narrower than the other bogies, it has more space to negotiate the curve. Therefore, it is likely that the track gauge does not affect this bogie as much as the others.

Tables 5 and 6 show the results of the calculated derailment coefficient and the angle of attack for different freight wagon bogies. The results are taken from the same passes that gave the highest lateral force values presented in Table 2.

Table 5. (Left) *Y/Q* derailment coefficient for the forces in measurement section 1 (wide gauge curve); (right) *Y/Q* derailment coefficient for the forces in measurement section 2 (narrower gauge curve) – outer wheel of the leading wheelset negotiating the curve. UL represents empty wagon and L represents loaded wagon. The scale of the colours is 0 (green) – 0.5 (orange) – 1 (red)

Y/Q, wide gauge curve					*Y/Q*, narrower gauge curve				
Bogie Type	5 km/h	15 km/h	25 km/h	35 km/h	Bogie Type	5 km/h	15 km/h	25 km/h	35 km/h
$K14_{UL}$	0.18	0.16	0.22	0.29	$K14_{UL}$	0.15	0.10	0.18	0.27
$K16_{UL}$	0.13	0.13	0.20	0.23	$K16_{UL}$	0.36	0.3	0.43	0.44
$K17_{UL}$	0.55	0.53	0.50	0.43	$K17_{UL}$	0.63	0.68	0.67	0.71
Two-axle$_{UL}$	0.32	0.26	0.38	0.40	Two-axle$_{UL}$	0.47	0.38	0.48	0.55
$K16_{L}$	0.12	0.13	0.18	0.28	$K16_{L}$	0.45	0.47	0.5	0.56
$K17_{L}$	0.45	0.41	0.40	0.40	$K17_{L}$	0.44	0.52	0.55	0.55
$Y25_{L}$	0.64	0.54	0.49	0.51	$Y25_{L}$	0.52	0.51	0.49	0.46
18-100$_{L}$	0.51	0.51	0.53	0.48	18-100$_{L}$	0.46	0.51	0.51	0.51
Two-axle$_{L}$	0.21	0.27	0.30	0.32	Two-axle$_{L}$	0.52	0.36	0.34	0.44

Table 6. (Left) Angle of attack in measurement section 1 (wide gauge curve); (right) Angle of attack in measurement section 2 (narrower gauge curve) – outer wheel of the leading wheelset negotiating the curve. UL represents empty wagon and L represents loaded wagon (all numbers are in milliradians). The scale of the colours is 0 (green), –10 (orange) and –20 (red).

Angle of attack, mrad, wide gauge curve					**Angle of attack, mrad, narrower gauge curve**				
Bogie Type	**5 km/h**	**15 km/h**	**25 km/h**	**35 km/h**	**Bogie Type**	**5 km/h**	**15 km/h**	**25 km/h**	**35 km/h**
$K14_{UL}$	–0.27	–0.68	–0.03	0.76	**$K14_{UL}$**	–1.84	–1.19	–0.62	–2.81
$K16_{UL}$	–1.39	–1.71	–2.26	–1.56	**$K16_{UL}$**	–4.76	–2.75	–4.29	–3.30
$K17_{UL}$	–9.98	–8.72	–11.13	–10.40	**$K17_{UL}$**	–18.42	–11.48	–11.87	–15.62
Two-axle_{UL}	–3.98	–2.21	–2.94	–4.55	**Two-axle_{UL}**	–17.36	–3.74	–5.42	–8.81
$K16_{L}$	–0.51	–1.99	–1.69	–5.64	**$K16_{L}$**	–10.64	–8.59	–7.46	–12.25
$K17_{L}$	–7.22	–5.36	–4.87	–5.16	**$K17_{L}$**	–13.79	–11.52	–9.29	–12.71
$Y25_{L}$	–8.47	–5.22	–6.60	–5.56	**$Y25_{L}$**	–14.64	–13.20	–11.83	–9.20
18-100_{L}	–9.98	–11.54	–9.31	–11.85	**18-100_{L}**	–12.53	–10.78	–11.91	–10.94
Two-axle_{L}	–2.92	–3.08	–4.19	–3.96	**Two-axle_{L}**	–16.53	–5.72	–5.07	–10.83

The Y/Q derailment coefficient ratio was well within the defined limits for most of the freight wagons (Table 5). The unloaded K17 bogie had a Y/Q ratio close to the limit value of 0.8 for the forces measured in the narrower gauge curve (measurement section 2). The tests reported by Müller et al. (2001) indicate that the K17 bogie steers well due to its softer suspension and outperforms the Y25 bogie. However, the results obtained from the Kouvola measurements give an indication that this particular unloaded K17 bogie does not perform well. A possible explanation is due to the potential high rotational stiffness of these bogies that affect the steering properties of the bogie. The angle of attack for this unloaded K17 bogie was high, which could lead to the high lateral force that was seen in Table 2. Because of the high lateral force, the Y/Q-value also becomes high (Table 5). For the K17 bogie, the rotational stiffness of the bogie could explain its inability to radially align along the curve. In the wide gauge curve, there is sufficient space for steering, as evidenced by the values that are markedly less compared to the ones in the narrower gauge curve.

For some of the axles, the vertical load was distributed unevenly on the outer and inner rails of the loaded freight wagons. For instance, the leading axle of the trailing Y25 bogie at 35 km/h showed an imbalance of the vertical load, which tends to occur with the typical Y25 bogies due to suspension lockups.

According to the angle of attack measurement results, the narrower curve (measurement section 2) showed higher values than the wide gauge curve (measurement section 1), as seen from Table 6. Such high values in the tighter curve for the angle of attack provide an explanation for the higher magnitude of lateral forces. There is no clear dependency on the variation of the angle of attack with the vehicle velocity, but there are instances where the angle of attack does decrease with an increase in velocity. A small trend can be seen where the slowest velocity corresponds to higher values. It was also observed that the trailing axle of the bogie has an angle of attack closer to zero, and in some cases, a positive value, thereby confirming the typical steering behaviour of a bogie.

The empty K14 bogie performed very well with the least amount of force, and it also steered very well. Based on the video photography that was taken during the measurements under the wagons, the first wheelset of K14 bogies, unlike the other bogies, was never in a clear flange contact, which explained the lower forces. The loaded Y25 and 18-100 three-piece bogies performed quite similar to each other in the loaded condition. This may be due to the tight clearances present in the suspension arrangement of these bogies. The Y25 bogie has a stiff suspension arrangement with a tight longitudinal clearance that increases the stiffness of the wheelset, making it hard to undertake small radius curves. Boronenko et al. (2006) show that the 18-100 bogies with less longitudinal clearance have rather poor performance in tighter curves with higher flange wear and angle of attack values.

4. Simulations

Multibody dynamic simulations were performed using the Vampire Pro simulation software to understand the behaviour of the freight wagon bogies. The model used for running the simulations is a Vok-wagon with three-piece 18-100 bogies. The structure of the model is presented in Figure 6. The axle weight of the Vok-wagon model is 223 kN (loaded) and 54 kN (empty).

The 3-piece bogie consists of two side frames connected with a bolster. As these side frames are directly linked to wheelsets (no suspension), this bogie type has a high unsprung mass compared to other bogie types. The springs are located between the side frames and the bolster. Damping in this bogie type is based on friction wedges. The model is presented with more detailed information in Loponen et al. (2016).

Running scenario close to the curve radius at the Kouvola railway yard was developed, and a 5-metre transition zone was used for the 200-metre curve radius based on measurement data. Both empty and loaded conditions were tested, and a cant of –20 mm was used in the curve, as it represents the typical cant measured in the Kouvola narrower gauge curve. Simulations were made in a curve with a track gauge of 1530 mm, because based on measurement results, this measurement section was noticed to cause higher lateral forces than a wider track gauge.

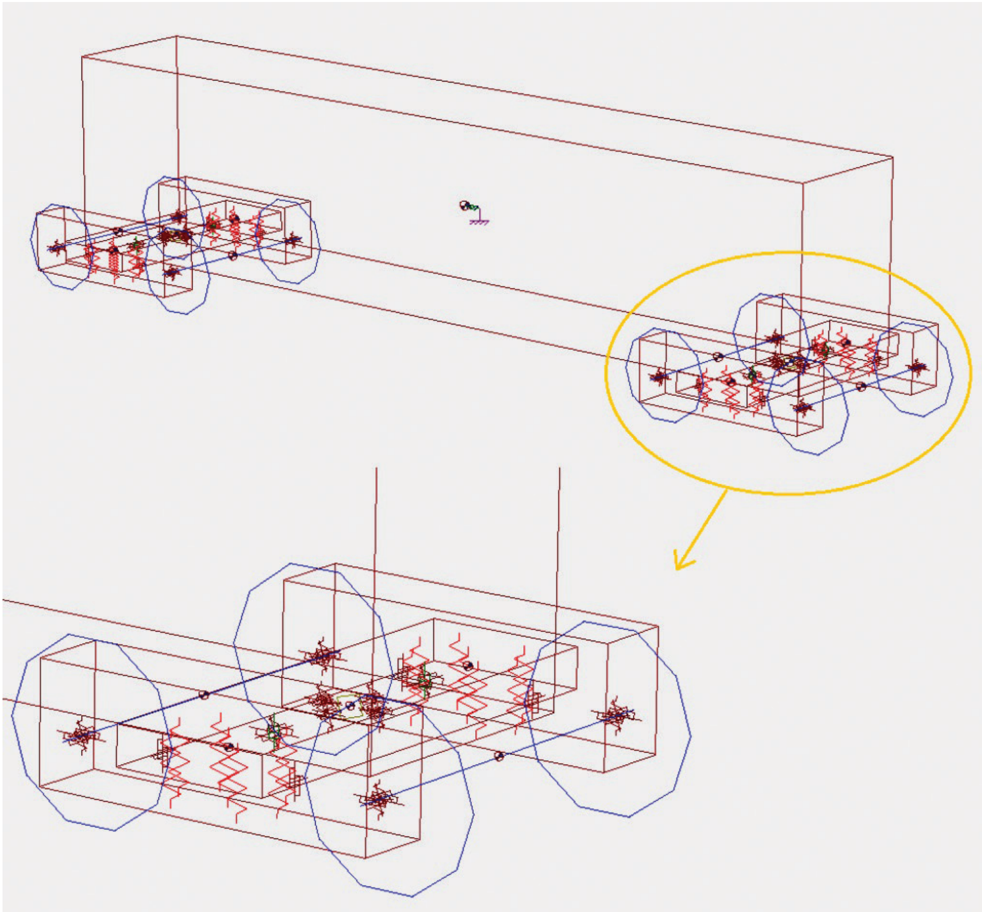

Figure 6. The structure of the Vok-wagon model with three-piece 18-100 bogies that was used in simulations. The bogie consists of two side frames, which are connected to the bolster in the middle of the bogie with springs and friction wedges

The wheel and rail profiles measured during Kouvola field measurements were used to simulate the wheel-rail interaction (Figure 7). The shape of the wheel profiles is pretty close to S1002 with 1.9 mm (outer wheel) and 3.8 mm (inner wheel) of side wear. The rail profiles are almost unworn 54E1-profiles.

The simulations indicate that the magnitude of lateral forces in the outer rail is smaller with empty wagons and increases with the increase in the axle loads. Partly due to the cant deficiency present along the curve radius, the loaded wagons impose higher lateral loads, and they also increase as the velocity increases (Figure 8).

Figure 8 shows that the simulated wheel lateral force increases significantly in the curved track section with both empty and loaded wagons. Correspondingly, the loaded wagon gives significantly higher lateral force values than the empty wagon. Especially with the loaded wagon, a higher velocity (35 km/h) gives higher lateral values than a lower velocity (5 km/h). The average value of the lateral force in the middle of the curve for the loaded wagon was 42.5 kN (5 km/h) and 48.8 kN (35 km/h). For the empty wagon, the corresponding values were 10.7 kN (5 km/h) and 12.5 kN (35 km/h). The average value was calculated for a distance of 100 m (from 170 m to 270 m). The maximum values of the measured lateral forces (loaded Vok-wagon, 18-100 bogie) are higher than the average simulated values. The differences between the measurement values and the simulation values might be due to the track model that was used in the simulations. The condition of the track that was used in simulations was likely better than the condition of the real measured track. The exact geometry of the real track was not measured, so it was not possible to use that data in the simulations.

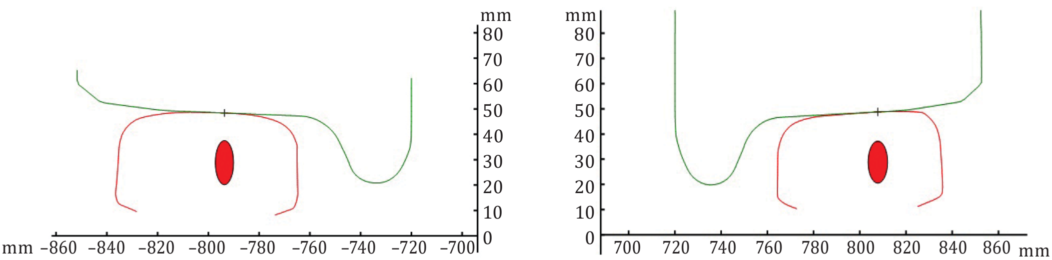

Figure 7. Rail profiles measured in the Kouvola narrower gauge curve and wheel profiles of the 18-100 bogie measured in Kouvola

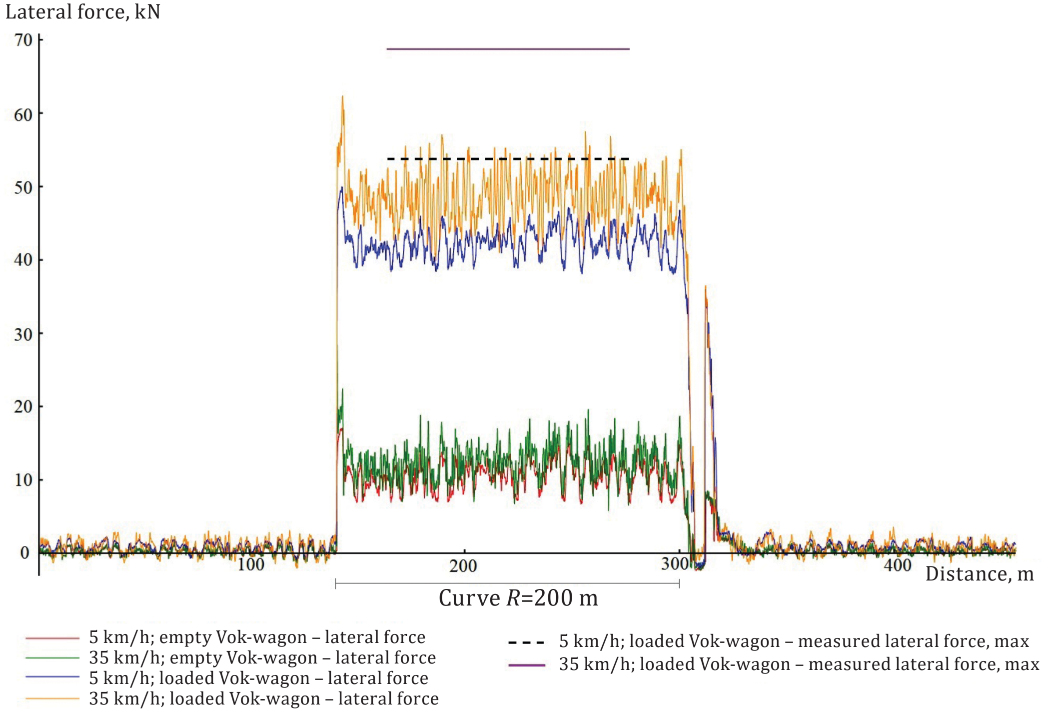

Figure 8. Lateral wheel force of the empty and loaded Vok-wagon with an 18-100 bogie, first wheelset and outer rail, velocity 5 km/h (empty red, loaded blue) and 35 km/h (empty green, loaded orange), curve R = 200 m. The maximum value of the measured Vok-wagon lateral force is shown with dashed black line (5 km/h) and with purple line (35 km/h). The curve starts at s = 140 m and ends at s = 300 m

Figure 9 shows how the wagon weight and velocity affect the Y/Q coefficient along the curve. Y/Q describes the derailment risk of the wagon, and a ratio above 0.8 can be considered a potential derailment risk.

The effect of a small radius curve on the derailment risk can be seen clearly in Figure 9. The Y/Q coefficient increases significantly in the curve, and with the empty wagon, the ratio is high at the beginning of the curve and even exceeds the value of 0.8 at a velocity of 35 km/h. However, with the loaded wagon, the value is not high enough to cause a realistic derailment risk. Also, the effect of velocity on the Y/Q coefficient was almost negligible with the loaded wagon. It is important to notice that with lighter wagons, the derailment risk was significantly higher than with heavier wagons. During the curve, the maximum value of the Y/Q ratio for the empty wagon was 0.66 (5 km/h) and 0.90 (35 km/h), and for the loaded wagon, 0.44 (5 km/h) and 0.49 (35 km/h). Also, in the Kouvola measurements, the highest Y/Q ratio occurred with an empty

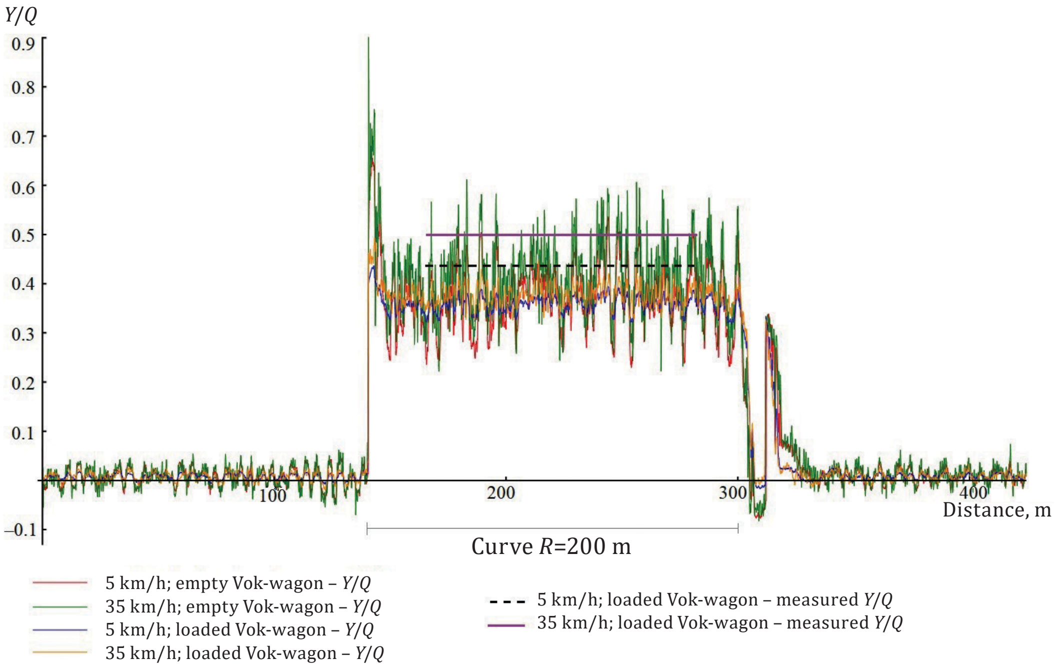

Figure 9. Y/Q coefficient of the empty and loaded Vok-wagon with an 18-100 bogie, first wheelset and outer rail, velocity 5 km/h (empty red, loaded blue) and 35 km/h (empty green, loaded orange), curve R = 200 m. The value of the measured Vok-wagon Y/Q is shown with dashed black line (5 km/h) and with purple line (35 km/h). The curve starts at s = 140 m and ends at s = 300 m

wagon. This type of small radius curve with only a short transition zone, and with the outer rail settled below the inner rail (negative cant), can be very risky regarding the derailment potential, especially for empty wagons. The measured Y/Q values of the loaded Vok-wagon were a bit higher than the simulated values. The measured values, however, were quite close to the simulated ones.

The angle of attack is also an important parameter in evaluating the derailment risk, and a small radius curve has a major influence on that value (Figure 10). The increase in the angle of attack value was considerably high during the curved track section, and the maximum value was always at the beginning of the curve.

Figure 10 shows that the velocity, however, has little influence on the angle of attack, which was also noticed from the field measurement results. The angle of attack is slightly bigger with the loaded wagon compared to the empty wagon during the whole curve. In the case of the loaded Vok-wagon shown in Figure 10, the values of the angle of attack were very close to the simulated values.

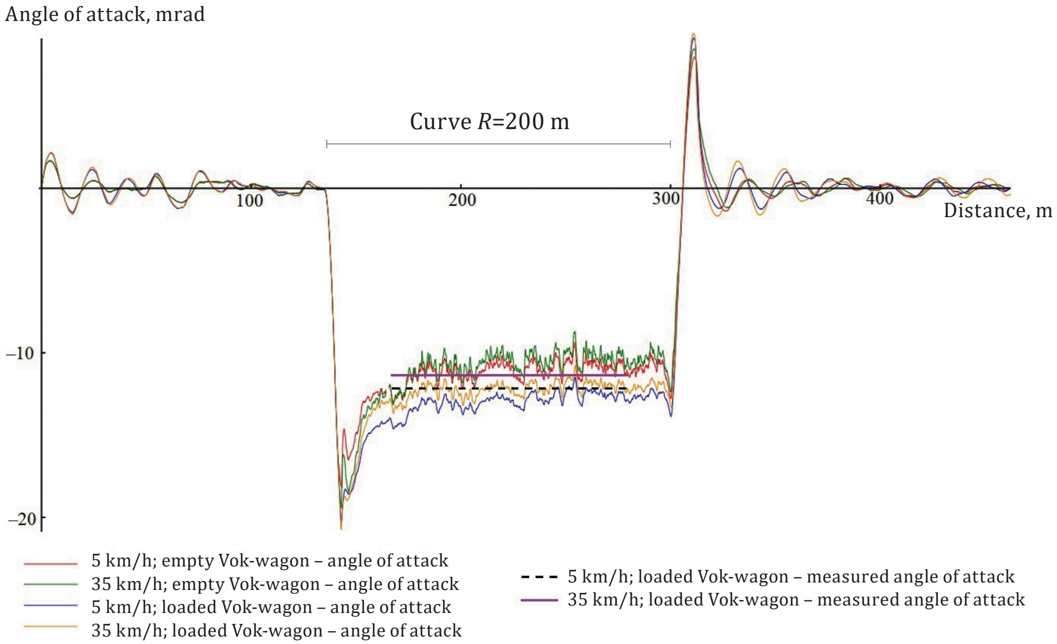

Figure 10. Angle of attack, first wheelset, empty and loaded Vok-wagon with an 18-100 bogie, velocity 5 km/h (empty red, loaded blue) and 35 km/h (empty green, loaded orange), curve R = 200 m. The value of the measured Vok-wagon angle of attack is shown with dashed black line (5 km/h) and with purple line (35 km/h). The curve starts at s = 140 m and ends at s = 300 m

In a small radius curve, a contact between the wheel flange and the rail is typical. The flange contact can be evaluated with the help of flange Tγ (Taugamma)-values in simulations (Figure 11). The Tγ-value describes the energy available for wear in wheel-rail contact, and the unit is J/m (or N).

The curve starts at s = 140 m, and at that point, the Tγ-value immediately increases (Figure 11). The value remains high until the curve ends at s = 300 m. This result means that the first wheelset has a flange contact throughout the curve, and this phenomenon occurs with both velocities (5 km/h and 35 km/h) and both wagons, empty and loaded. As the flange Tγ-values are higher with the loaded wagon, a heavier wagon causes more wear in wheel-rail flange contact than an empty wagon. In addition to the flange Tγ-values, the Tγ-values of tread contact were also examined. Overall, the tread values were clearly lower than the flange values, and the heavier wagon caused more wear than the empty wagon in tread contact as well.

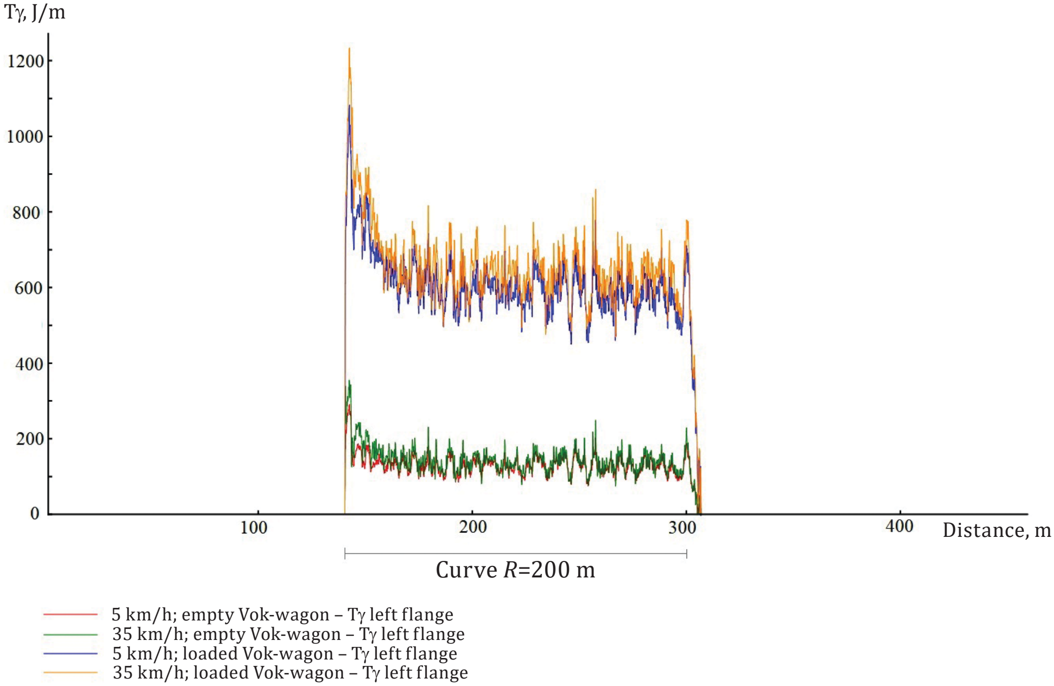

Figure 11. Tγ-values in flange contact (outer rail, first wheelset), empty and loaded Vok-wagon with an 18-100 bogie, velocity 5 km/h (empty red, loaded blue) and 35 km/h (empty green, loaded orange), curve R = 200 m. The curve starts at s = 140 m and ends at s = 300 m

The simulations were also conducted with wider track gauges (G = 1535 mm and G = 1540 mm) to get the impression of how much the track gauge affects the results. In all the simulation cases with the Vok-wagon (18-100 bogie), the track gauge had a minor effect on the wheel lateral forces, Y/Q values, angle of attack values, and Tγ-values. This result is likely due to the structure of the 18-100 bogie (narrow wheelset) and the unavoidable flange contact that appeared in all simulation cases. However, the track gauge only had a small effect on the measurement values in the case of the real 18-100 bogie as well, so the relationship between lateral force and track gauge probably depends heavily on the bogie type.

A numerical comparison of the simulations and the field measurement results for the loaded 18-100 bogie in the narrower gauge curve is shown in Table 7. The 95th percentile and average values for a distance of 100 m in the middle of the curve section are presented. For the loaded 18-100 bogie, the measurement data and simulation results were quite close to each other. Although it is impossible to exactly replicate the running conditions along with the deterioration of the track and the wagon, these comparisons give a better overall understanding and help improve the simulation models. The comparison could only be made with the loaded 18-100 bogie, as it was not possible to get the empty configuration for the field measurement tests.

As seen in Table 7, the observations were the same with both the measurement results and simulation results: when the velocity increases, the lateral forces climb higher, and the angle of attack becomes smaller. The 95th percentiles of the simulation results were quite close to the measurement results, especially with the angle of attack values. It should be noted though that individual variations with different wagons of the same wagon type do exist, and these measurements only had one wagon with the 18-100 bogie.

Table 7. Comparison of the lateral force, vertical force, *Y*/Q, and angle of attack (AOA) measurement and simulation results for the 18-100 bogie. Loaded condition, worn wheel and rail profiles

18-100 Loaded	**Measurement data**		**95% (simulation)**		**Average (simulation)**	
	5 km/h	**35 km/h**	**5 km/h**	**35 km/h**	**5 km/h**	**35 km/h**
18-100$_L$ lateral force, kN	53.98	69.75	45.54	54.36	42.49	48.76
18-100$_L$ vertical force, kN	117.60	136.70	119.84	132.59	118.03	128.32
18-100$_L$ Y/Q	0.46	0.51	0.38	0.41	0.36	0.38
18-100$_L$ AOA, mrad	–12.53	–10.94	–12.16	–11.56	–12.93	–12.20

Table 8. Comparison of the lateral force, *Y*/*Q*, and angle of attack (AOA) results with unworn and worn profiles for the 18-100 bogie. Loaded condition, average values

18-100 Loaded	Measurement data		Unworn profiles		Worn profiles	
	5 km/h	35 km/h	5 km/h	35 km/h	5 km/h	35 km/h
$18\text{-}100_L$ lateral force, kN	53.98	69.75	46.26	52.14	42.49	48.76
$18\text{-}100_L$ vertical force, kN	117.60	136.70	118.62	127.17	118.03	128.32
$18\text{-}100_L$ Y/Q	0.46	0.51	0.39	0.41	0.36	0.38
$18\text{-}100_L$ AOA, mrad	–12.53	–10.94	–11.22	–10.67	–12.93	–12.20

A comparison was also made to see the effect of the wheel and rail profile shapes on the results. Table 8 shows the simulation results for unworn wheel and rail profiles compared to the measured worn profiles.

As seen in Table 8, unworn profiles gave slightly higher lateral forces and Y/Q values than worn wheel and rail profiles. However, the angle of attack was lower with unworn wheel and rail profiles, which was likely due to the smaller rail clearance value. Thus, wear in rail and wheel profiles may reduce the contact forces between the wheel and the rail.

Conclusions

The performance of the freight wagon bogies depends on several parameters, such as the structure of the bogie, wagon weight and velocity, wheel and rail profiles, condition of the suspension system, and bogie rotational stiffness. In this paper, an effort was made to study the behaviour of different freight wagon bogies by measuring and simulating the wheel-rail forces and the angle of attack, especially in small radius curves like the one in Kouvola. The selected curve (R = 200 m) in the Kouvola railway yard has a variable cant profile with the outer rail lower than the inner rail (varying between 0 to 25 mm) and with varying track gauges (a difference of 5 mm) between the measurement sections, thereby adding complexity to the testing conditions.

The following conclusions can be drawn from this study:

1. The running safety is best analysed by predicting the possibility of derailment, and, thus, the Y/Q derailment coefficient was calculated. In the measurements, the derailment coefficient was well within the defined limits for almost all the freight wagon bogies except for the empty K17 bogie, which was close to the limit value in the narrower gauge curve region. A high rotational

stiffness of these freight wagons could be a potential reason for the inability of the wagon to steer, giving rise to a high amount of lateral forces. However, even higher Y/Q values were obtained through simulations at the beginning of the curve, as the empty Vok-wagon with an 18-100 bogie gave a value of 0.90 at a running velocity of 35 km/h. A small radius curve like the one used in measurements and simulations with only a short transition zone, and with the outer rail settled below the inner rail (negative cant), can be very risky regarding the derailment potential, especially for empty wagons.

2. With some bogies, the track gauge plays an important role as the lateral forces were mainly lower in the wider section (measurement section 1) when compared to the narrower section of the curve (measurement section 2). The magnitude of lateral forces imposed by the outer wheel of the leading wheelset for the loaded condition was greater than for the empty condition. In the field measurements, the magnitude of lateral forces reached its maximum at the highest running velocity that was used (35 km/h). In the measurements, the K16 bogie had the highest amount of lateral forces with values going up to 76 kN in the narrower gauge curve section. Overall, the lateral forces were usually lower with a wider track gauge. Based on these results, it would be beneficial to use a wider track gauge in small radius curves to make the curve negotiation easier for some bogie types.
3. The angle of attack measurement provides information on the steering ability of different freight wagon bogies. The angle of attack was higher for the leading axles on the outer rail and specifically for the lower velocity running condition in the narrower gauge curve. The empty K17 bogie had the highest angle of attack, suggesting that the position of the wheelset in the curve was far from the optimal position. Simulations revealed that vehicle speed did not have a significant influence on the angle of attack value overall. A smaller velocity gave a slightly higher value for the angle of attack in simulations as well.
4. Simulations provide a broader perspective in analysing the measurement results. The results from simulations show that the values for the loaded 18-100 bogie were quite close to the measured ones. $T\gamma$-values for the 18-100 bogie were also obtained. They revealed that the 18-100 bogie had unavoidable flange contact while running along a curve, which led to a high rate of wear in wheel-rail contact.

The field measurements provide valuable information about the actual running behaviour of the freight wagon bogies. A plan is devised to build simulation models for other freight wagon bogies as a follow-up to this initial project in the future. Such models help in understanding the loading behaviour between the wheel and the rail, and the amount of damage caused to the tracks can be estimated.

Acknowledgements

This research was made in collaboration with the Finnish Transport Infrastructure Agency and the Finnish Railway operators. The research would not have been possible without their support. The authors would also like to thank Marko Happo and Tommi Rantala for their valuable help during the field measurements.

Funding

The research was funded by the Finnish Transport Infrastructure Agency, Finland (FTIA) and Tampere University. The collaboration between the FTIA and Tampere University is much appreciated in implementing the research activity.

REFERENCES

Arias-Cuevas, O., Li, Z., Popovici, R. I., & Schipper, D. J. (2010). Simulation of curving behaviour under high traction in lubricated wheel-rail contacts. *Vehicle System Dynamics*, *48*(Sup1), 299–316. https://doi.org/10.1080/00423111003746132

Boronenko, Y., Orlova, A., & Rudakova, E. (2006). Influence of construction schemes and parameters of three-piece freight bogies on wagon stability, ride and curving qualities. *Vehicle System Dynamics*, *44*(Sup1), 402–414. https://doi.org/10.1080/00423110600872341

Diana, G., Bruni, S., Di Gialleonardo, E., Corradi, R., & Facchinetti A. (2016). A study of the factors affecting flange-climb derailment in railway vehicles. *Proceedings of the 3rd International Conference on Railway Technology*. https://www.ctresources.info/ccp/download/XDYNA81C5OSDRUOJ.pdf

Finnish Transport Infrastructure Agency. (2024, January 24). *Rautateiden verkkoselostuksen karttapalvelu.* https://suomenvaylat.vayla.fi/?lang=en

Hiensch, M., Burgelman, N., Hoeding, W., Linders, M., Steenbergen, M., & Zoeteman, A. (2018). Enhancing rail infra durability through freight bogie design. *Vehicle System Dynamics*, *56*(10), 1532–1551. https://doi.org/10.1080/00423114.2017.1421766

Jönsson, P-A. (2007). *Dynamic vehicle-track interaction of European standard freight wagons with link suspension* [Doctoral dissertation, KTH, Aeronautical and Vehicle Engineering]. Stockholm, Sweden. https://www.diva-portal.org/smash/get/diva2:12382/FULLTEXT01.pdf

Loponen, T-R., Salmenperä, P., & Nurmikolu, A. (2016). *Liikkuvan kaluston ja raiteen välinen vuorovaikutus ja sen dynaaminen mallinnus.* Liikenneviraston tutkimuksia ja selvityksiä 14/2016. Liikennevirasto, Helsinki. 155 p. *In Finnish.*

Milković, D., Simić, G., Tanasković, J., Lučanin, V., & Radulović, S. (2017). Uncertainty of the wheel-rail angle of attack measurements using laser based wayside system. *FME Transactions*, *45*(1), 69–76. https://doi.org/10.5937/fmet1701069M

Milković, D., Simić, G., Tanasković, J., Jakovljević, Ž., & Lučanin, V. (2015). Experimental and numerical determination of the wheel-rail angle of attack. *Facta Universitatis Series Mechanical Engineering*, *13*(2), 123–131.

Müller, C. (2001). *Höhere Radsatzlasten bei geringerer Beanspruchung?* Drehgestell. Eisenbahningenieur, 52, 7/2001, 38–40.

Orvnäs, A., Andersson, E., & Persson, R. (2007). *Development of track-friendly bogies for high speed. A simulation study.* KTH, Grönatåget. Stockholm.

Powell, A.F., & Gräbe, P. J. (2017). Exploring the relationship between vertical and lateral forces, speed and superelevation in railway curves. *Journal of the South African Institution of Civil Engineering*, *59*(3), 25–35. https://doi.org/10.17159/2309-8775/2017/v59n3a4

RISSB. (2021). *Good practice for the management of wheel squeal.* White paper, Rail Industry Safety and Standards Board, Australia.

Solčanský, S. (2021). Lenoir friction damper and its applications. *Transportation Research Procedia*, *55*, 744–751. https://doi.org/10.1016/j.trpro.2021.07.176

Stichel, S. (1999). On freight wagon dynamics and track deterioration. *Proceedings of the Institution of Mechanical Engineers, Part F: Journal of Rail and Rapid Transit*, 213(4), 243–254. https://doi.org/10.1243/0954409991531182

Thompson, D. (2009). *Railway noise and vibration. Mechanisms, Modelling and Means of Control.* Elsevier Science. UK. https://doi.org/10.1016/B978-0-08-045147-3.X0023-0

UIC 518. (2005). *Testing and approval of railway vehicles from the point of view of their dynamic behaviour – safety – track fatigue – ride quality*. UIC.

Vollebregt, E., Six, K., & Polach, O. (2021). Challenges and progress in the understanding and modelling of the wheel-rail creep forces. *Vehicle System Dynamics*, *59*(7), 1026–1068. https://doi.org/10.1080/00423114.2021.1912367

Weilguny, R., Leitner, M., Brunnhofer, P., & Pospischil, F. (2024). Investigation of dynamic gauge widening in small radius curves and its impact on lateral wheel-rail contact forces. *Vehicle System Dynamics*, *62*(8), 2112–2137. https://doi.org/10.1080/00423114.2023.2276762

Wu, H., & Wilson, N. (2006). *Handbook of railway vehicle dynamics. Railway vehicle derailment and prevention*. Edited by S. Iwnicki. CRC Press, UK.